^{18}FDG PET and Ultrasound Echolucency in Carotid Artery Plaques

Martin Græbe, MD,* Sune F. Pedersen, MSc,† Liselotte Højgaard, MD, DMSc,‡
Andreas Kjær, MD, PhD, DMSc,†‡ Henrik Sillesen, MD, DMSc*

Copenhagen, Denmark

OBJECTIVES The objective was to evaluate inflammation in echolucent carotid artery plaques.

BACKGROUND Ultrasound echolucency of carotid artery plaques has been proven to differentiate patients at high risk of stroke. On the other hand, positron emission tomography (PET) of plaques with the use of [^{18}F]-fluorodeoxyglucose (FDG) identifies highly inflamed plaques, and the combination of molecular imaging and morphology could improve identification of vulnerable plaques.

METHODS A total of 33 patients with cerebrovascular symptoms and carotid artery plaques were included prospectively for ultrasound and PET imaging. Plaque standardized gray scale medians (GSM) were measured in longitudinal ultrasound images to quantitate echolucency, and GSM values were compared with FDG PET uptake quantified by maximum standardized uptake values (SUV). Symptomatic plaques were compared with contralateral carotid artery plaques considered asymptomatic, and in 17 symptomatic patients, endarterectomized plaque specimens were analyzed for CD68 expression.

RESULTS There was a negative correlation between GSM and FDG SUV (r = −0.56, p < 0.01). Whereas echo-rich plaques tended to show low FDG uptake, echolucent plaques ranged from high to low inflammatory activity, as depicted with PET. Quantitative FDG SUV differentiated asymptomatic from symptomatic plaques, whereas GSM values did not. There was a positive correlation between CD68 expression and FDG uptake (r = 0.50, p = 0.04).

CONCLUSIONS Our results substantiate previous findings of an association between plaque FDG uptake and inflammation. Echolucent plaques exhibit a wide range of inflammatory activity, whereas echorich plaques show little inflammation. FDG PET may be useful for further stratification of echolucent plaques being either active (vulnerable) or inactive. (J Am Coll Cardiol Img 2010;3:289–95) © 2010 by the American College of Cardiology Foundation

several subgroups of both patient- and plaque-specific risk factors have been identified in an effort to improve the stratification of patients at risk of a primary or secondary stroke. Besides medical treatment, the current prophylactic treatment standard is carotid endarterectomy, which is reserved for a limited number of patients only, and current stratification regimens for operation are only on the basis of the size of the plaque (degree of stenosis) and time since last neurological event, if any (1). The risk of cerebrovascular events (stroke, transitory ischemic attack, or eye-emboli [amaurosis fugax]) is considerable in patients with carotid artery stenosis in general, and the risk of a recurrent event from symptomatic plaques is even greater (2,3).

The distinct difference in risk profile for asymptomatic and symptomatic plaques probably reflects that vulnerable plaques are greatly overrepresented among symptomatic plaques. Besides inflammation, several morphological features that can be assessed by ultrasound characterize the vulnerable plaque, and one of the most substantiated predictors of recurrent events is plaque echolucency. Its use as a clinical routine method is limited because advanced computerized image standardization, used in this study, is necessary to overcome the subjectivity (4,5). It has been shown that echolucent plaques are associated with an increased risk of ipsilateral events and increased presence of plaque macrophages (6–8).

New imaging modalities are emerging, and positron emission tomography (PET) of atherosclerosis with the use of the radiotracer [^{18}F]-fluorodeoxyglucose (FDG), in which glucose metabolism within plaques can be assessed with high sensitivity, has been suggested as a diagnostic method for risk stratification (9–11). High FDG uptake in carotid artery plaques is associated with an abundant presence of macrophages and molecular gene up-regulation of enzymes known to degrade the cellular matrix of vulnerable plaques (12–14). Hence, FDG PET is believed to depict inflammation in atherosclerotic carotid lesions, and this noninvasive molecular imaging method thus provides information that cannot be assessed with the use of ultrasound.

The aim of our study was to evaluate the association between carotid plaque ultrasound echogenicity and the presence of inflammation depicted with FDG PET. To do so, results from the 2 imaging modalities were compared by correlation. Plaque

gene-expression of CD68, a marker of macrophage presence, was used in a subgroup of patients to investigate the association between inflammation and FDG uptake, and the ability of FDG PET to discriminate between asymptomatic and symptomatic plaques was used as a surrogate marker of both risk assessment and inflammatory activity.

METHODS

Patients. A total of 33 patients referred from neurologists for carotid ultrasound investigation after symptoms of cerebral ischemia were prospectively included. In these patients, a total of 21 asymptomatic plaques and 34 symptomatic plaques were found. The term "plaque" is used in this report for all atherosclerotic lesions independent of degree of stenosis. Eligible symptoms were stroke, transitory ischemic attack, or momentary monocular blindness and an ipsilateral carotid artery plaque. If a contralateral plaque was present, it was included as an asymptomatic plaque. In all cases, the ipsilateral carotid plaque was considered the reason for cerebral ischemia; that is, no patients had atrial fibrillation, and all patients underwent computed tomography (CT) scans to rule out intracranial etiology for the cerebral symptoms.

Two patients had bilateral symptomatic plaques, and 1 had bilateral asymptomatic plaques because symptoms were nonhemispheric (vertigo). Patients were included after an overnight fast, and information on common risk factors (age, sex, diabetes, smoking, hypertension) and medical history was

Table 1. Patient Data

|	
Sex, male	25 (75.8)
Antihypertensive medication, yes	27 (81.8)
Current smoking, yes	13 (39.4)
Diabetes, yes	4 (12.1)
Age, yrs	68 (63.5–75.5)
Time since last symptom, days	46 (21.5–72.5)
Plasma levels	7.2 (5.8–8.2)
Leukocytes, billion/l	7.2 (5.8–8.2)
CRP, mg/l	3 (1.2–5.8)
Cholesterol, mmol/l	4.3 (3.5–4.7)
LDL, mmol/l	2.3 (1.7–2.6)
HDL, mmol/l	1.5 (1.2–1.7)
Triglycerides, mmol/l	1.1 (1.0–1.4)
Creatinine, μmol/l	89 (71.5–102.0)
Glucose, mmol/l	5.6 (5.2–6.2)

Scale variables are presented as median with interquartile range and categorical variables with number and percentage, n = 33.
CRP = C-reactive protein; HDL = high-density lipoprotein; LDL = low-density lipoprotein.

obtained, along with blood samples. Exclusion criteria were insulin-treated diabetes, a blood glucose measurement before FDG injection >8 mmol/l, vasculitis, impaired kidney function (creatinine >125 μmol/l), and treatment with immunomodulating or anti-inflammatory drugs due to inflammatory or oncologic disease. An ultrasound investigation and a PET/CT scan were performed the same day. A total of 17 patients accepted carotid endarterectomy, which was performed the following day. All patients who underwent surgery had a plaque causing >50% stenosis and ipsilateral hemispheric symptoms within the past 3 months. All patients provided written informed consent, and the national ethics committee approved the study (ref. no. 0120065513).

Ultrasound. Ultrasound was performed with a linear 9-3 MHz transducer on both carotid arteries (iU22 Ultrasound System; Philips Ultrasound, Bothell,

Washington). A vascular pre-setting was chosen before each investigation to ensure uniform recordings with maximum dynamic range (60 dB), a mechanical index of 1.1, and a linear post-processing curve. Gain was set just below visual presence of echoes in blood. B-mode digital video sequences (frame rates of 28 to 42 Hz) of the plaque were recorded while sweeping the plaque in longitudinal, circumferential, and transverse directions with and without color duplex. Degree of stenosis was determined according to a Doppler assessment of peak systolic flow (15).

CT angiography and ultrasound video recordings were thoroughly compared, and 1 single ultrasound image representing a longitudinal cut through the entire length of the plaque was chosen for gray scale median (GSM) analysis. The image was loaded directly in DICOM format to imaging software (Adobe Photoshop CS4 Extended; Adobe Systems
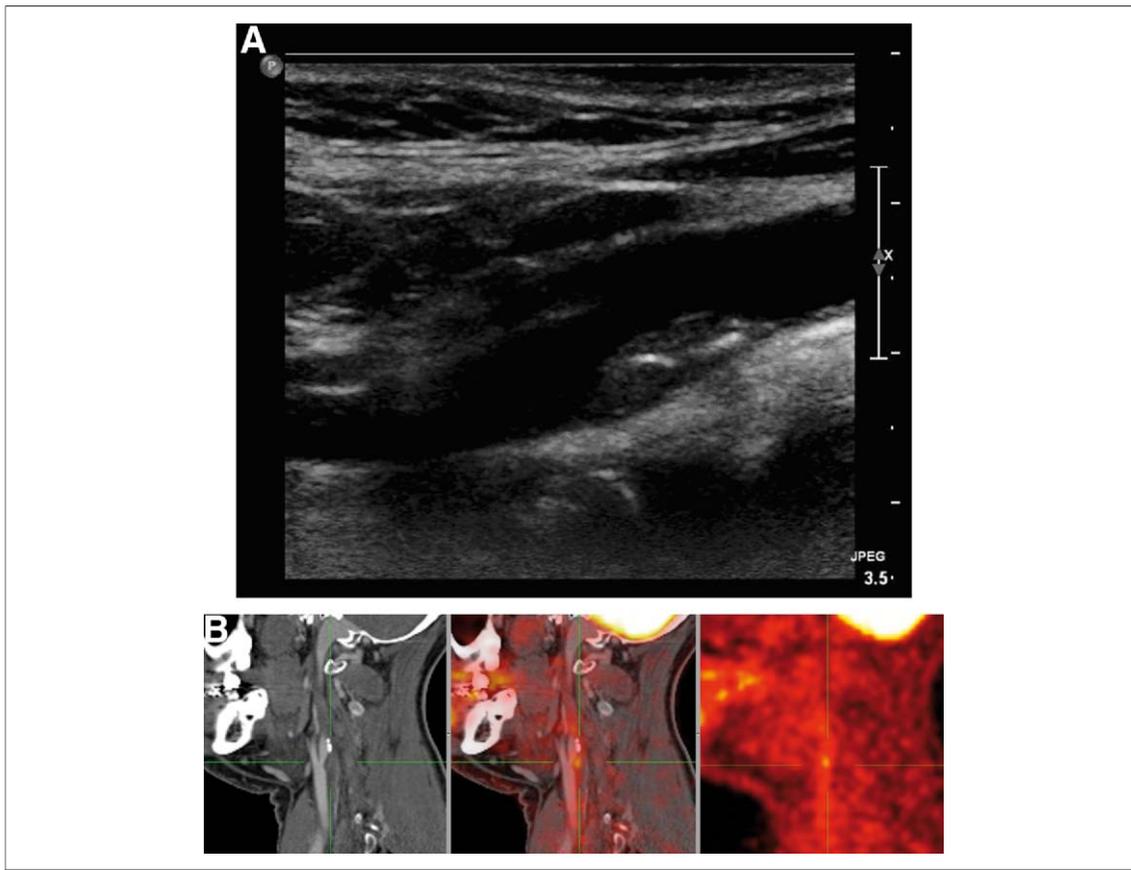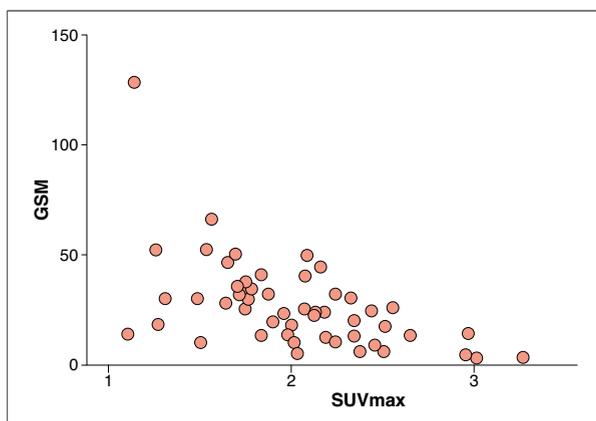

Figure 1. Ultrasound and PET in Carotid Artery Disease

Examples of ultrasound imaging and [18F]-fluorodeoxyglucose (FDG) positron emission tomography (PET)/computed tomography (CT) in a male patient (50-years-old) with moderate stenosis (50% to 60%) and transitory ischemic attack 13 days before investigation. **(A)** Longitudinal ultrasound image demonstrating a heterogeneous plaque with a smooth surface and a gray scale median of 24. Note the shadowing in the internal carotid artery just cranial **(left)** of the plaque corresponding to calcified areas also identified on the CT. **(B)** CT **(left)**, the fused PET/CT **(middle)**, and FDG PET **(right)** reveal inflammation corresponding to the suspected culprit lesion (just below the calcified areas). The patient was offered surgery but declined and was discharged with medical treatment alone.

Inc., Seattle, Washington) for built-in GSM measurements. Image standardization was performed by applying a black and white adjustment layer, 256-point gray scale, followed by a new curve adjustment layer where lumen was set to black, output 0 to 5, and transducer near adventitia to near white, output 185 to 195 (4). The plaque was delineated with a freehand tool, omitting areas with shadowing from calcified areas, and a GSM was read from the entire delineated area.

PET/CT. A PET/CT (Siemens BioRad 16; Siemens, Berlin, Germany) was performed 3 h after intravenous injection of 400 MBq of FDG. Patients had been fasting for at least 6 h before injection. With the patient's head placed in a head holder, dental prosthesis removed, and arms aligned to the side, 3 fields of view (15 cm) PET was performed in 3 dimensions for 4 min each. A low-dose CT (120 keV, 50 mAs) for attenuation correction preceded the PET scan. After the PET acquisition, a contrast-enhanced (100 ml of intravenous Optiray [iodine 300 mg/ml]; Mallinckrodt Inc., Hazelwood, Missouri) CT arteriography was made (120 keV, 200 mAs). Images were reconstructed using the 2-dimensional ordered subset expectation maximization with 8 iterations, 4 subsets, 3-mm Gaussian filtering, a voxel size of $256 \times 256 \times 55$ and axial slice thickness of 2 mm (Siemens Navigator workstation, SynGo Somaris/5 software; Siemens).

From the CT angiography, the carotid arteries were identified and delineated with an oval region of interest if plaques were present. Attenuation-corrected PET images were fused with the CT, and manual fusion corrections were made in 3 planes (2-dimensional orthogonal multiplanar reformations) with the use of brain, glands, vocal chords, and spine as anchoring points (OsiriX version 3.5.1 64-bit; OsiriX Imaging Software, Geneva, Switzerland). Consecutive readings of maximum standardized uptake values (SUVmax) (SUVmax = maximum counts in region of interest $\times$ patient weight/decay [time] corrected dose) were made for the entire plaque length (several trans-axial images) and expressed as a single average value.

Plaque gene-expression analysis. Plaques were removed during carotid endarterectomy for quantitative polymerase chain reaction (PCR) analysis of CD68 gene up-regulation as previously described (13). In brief, plaques were sliced transversally in 2-mm slices and treated with RNALater (Applied Biosystems, Foster City, California). After RNA extraction (Agilent 2100 Bioanalyzer; Agilent Technologies Inc., Santa Clara, California) and reverse transcriptase PCR (AffinityScriptQPCR cDNA Synthesis Kit; Stratagene, La Jolla, California), the quantitative PCR was performed with the use of the TaqMan Assay (Applied Biosystems). CD68 up-regulation in the plaques was expressed relative to mathematically pooled reference material consisting of samples of the superior thyroid artery excised from the same patients during endarterectomy. All slices were analyzed and averaged for each plaque.

Statistics. The GSM values and FDG uptake were correlated and expressed with a Spearman correlation coefficient (r). A Mann-Whitney U test was performed as a t test between asymptomatic and symptomatic plaques. Because several plaques came from the same patient (bilateral plaques), the assumption of independence was violated and, therefore a Wilcoxon signed rank test (paired comparison) was included to test whether FDG uptake differed within a subpopulation with bilateral plaques (n = 19 pairs, symptomatics with no contralateral plaque being excluded).

Comparisons of FDG uptake and GSM values between different subgroups of degree of stenosis (Fig. 4) were investigated with the use of the Kruskal-Wallis tests. The Fisher exact test was used to test differences in degree of stenosis between symptomatic and asymptomatic plaques. Because the degree of stenosis differed significantly between asymptomatic and symptomatic plaques, the effect

Figure 2. Association Between Echogenicity and FDG Uptake

Gray scale median (GSM) in a single longitudinal ultrasound image was compared with FDG PET uptake, quantified with maximum standardized uptake value (SUVmax), in the same carotid artery plaque. The FDG uptake was expressed as an average of all transverse PET slices (3 mm) that contained the individual plaque. The correlation was negative (r = −0.556, p < 0.0001), and the distribution suggested that echolucent plaques exhibit different degrees of inflammation (FDG uptake), whereas echorich plaques (high GSM) show relatively less inflammatory activity. Abbreviations as in Figure 1.

and interaction of these variables (size and symptoms) on FDG uptake were tested forwardly with a univariate F test in a general linear model with SUVmax as single dependent value. The SUVmax data were normally distributed, whereas GSM were not according to Shapiro-Wilk tests and histograms. The CD68 gene expression was normally distributed when log-transformed, and a correlation to SUVmax was made with the use of the Pearson correlation. Data were presented as medians with interquartile ranges, and $p < 0.05$ (2-sided) was considered significant for all statistical tests. Statistical calculations and graphics were made with SPSS version 16.0.1 for Mac (SPSS Inc., Chicago, Illinois) and Prism version 5.0b for Mac (GraphPad Software Inc., San Diego, California).

RESULTS

All patients had atherosclerosis and cerebrovascular symptoms, and therefore the entire population was considered at high risk for cardiovascular disease in general. Common risk factors and laboratory values for the patients are shown in Table 1. All patients received cholesterol-lowering drugs (statins) and antiplatelet medication at least 1 week before inclusion in the study.

Comparisons of echolucency and FDG uptake revealed that echolucent plaques exhibited a wide range of inflammation, whereas echorich plaques were depleted of PET-depicted inflammation. Examples of an ultrasound longitudinal single-slice and corresponding PET/CT scan from 1 patient are shown in Figure 1, and the negative association found between GSM and FDG uptake ($r = -0.556$, $p < 0.0001$) is shown in Figure 2.

FDG uptake was significantly lower in asymptomatic plaques compared with symptomatic plaques, whereas the numerical difference in GSM was not significant (Table 2). This finding was strengthened by a paired test including only patients
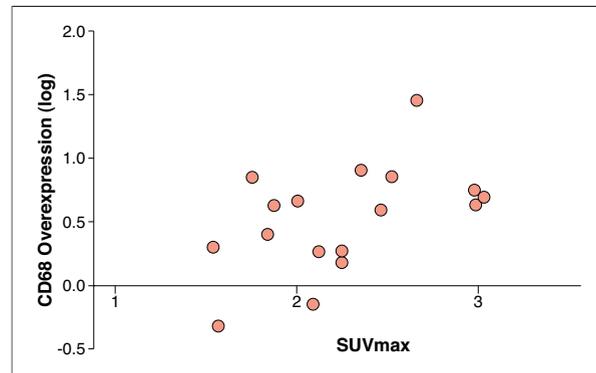
Figure 3. Association Between FDG PET Uptake and Inflammatory Activity

Average macrophage specific CD68 gene up-regulation from all 3-mm slices from the endarterectomized plaque was used as a marker of inflammatory activity. FDG uptake was quantified with SUVmax in a corresponding number of transverse PET slices containing the same plaque. Log-transformed gene upregulation was expressed relative to arterial reference tissue (0 is baseline) pooled from all patients. The correlation was positive ($r = 0.501$, $p = 0.041$), suggesting that FDG uptake depicts macrophage presence and, thus, inflammatory activity. Abbreviations as in Figures 1 and 2.

with bilateral plaques ($n = 19$) that also showed significant differences ($p = 0.023$) between asymptomatic plaques, SUVmax $= 1.907$ (1.714 to 2.181), and symptomatic plaques, SUVmax $= 2.020$ (1.714 to 2.335). Further evidence for the hypothesized association between FDG uptake and inflammation was found as FDG uptake correlated to CD68 expression in 17 endarterectomized symptomatic plaques ($r = 0.501$, $p = 0.041$) (Fig. 3).

The GSM did not correlate to CD68 expression ($p = 0.153$, not shown). Plaque size (degree of stenosis) differed between asymptomatic and symptomatic plaques (Table 3). However, regression analysis showed that for all plaques together, degree of stenosis was not an explanatory covariable for SUVmax ($p = 0.095$), nor did it interact with symptoms ($p = 0.220$) on FDG uptake values. Neither significant difference in SUVmax nor GSM values was observed between different degrees of stenosis (Fig. 4).

Table 2. Quantification in Asymptomatic and Symptomatic Plaques

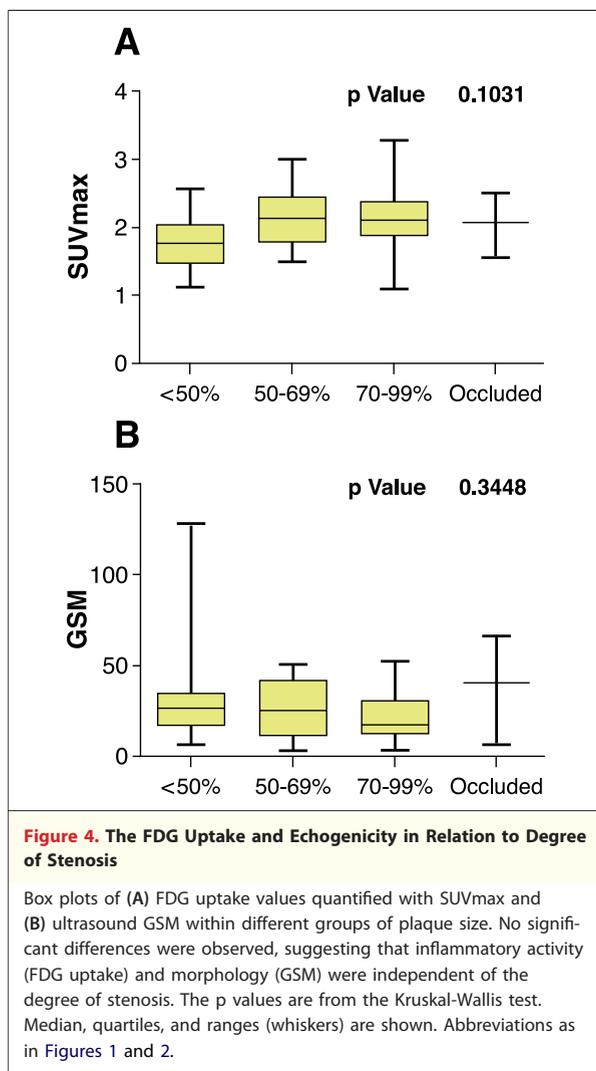|	SUVmax		GSM	
	n	Median (quartiles)	n	Median (quartiles)
Asymptomatic	21	1.847 (1.65–2.13)	21	24 (14–30)
Symptomatic	34	2.086 (1.76–2.78)*	32	22 (10–38)
p Value		0.041		0.610

Comparison of FDG PET (SUVmax) and ultrasound GSM characteristics of symptomatic and asymptomatic plaques. *p < 0.05 compared with asymptomatic.
FDG PET = [^{18}F]-fluorodeoxyglucose-positron emission tomography; GSM = gray scale median; SUVmax = maximum standardized uptake value.

Table 3. Degree of Stenosis and Symptom Status

Degree of Stenosis, %	Asymptomatic, n (%) (n = 21)	Symptomatic, n (%) (n = 34)
<50	14 (66.6)	3 (8.8)
50–69	1 (4.8)	10 (29.5)
70–99	6 (28.6)	18 (52.9)
Occluded	0	3 (8.8)

Count and column percent for different plaque size categories. Plaque size differed significantly between asymptomatic and symptomatic plaques, p < 0.001, in Fisher exact test.

Figure 4. The FDG Uptake and Echogenicity in Relation to Degree of Stenosis

Box plots of **(A)** FDG uptake values quantified with SUVmax and **(B)** ultrasound GSM within different groups of plaque size. No significant differences were observed, suggesting that inflammatory activity (FDG uptake) and morphology (GSM) were independent of the degree of stenosis. The p values are from the Kruskal-Wallis test. Median, quartiles, and ranges (whiskers) are shown. Abbreviations as in Figures 1 and 2.

DISCUSSION

The present data support a role for PET scans in potentially discriminating patients with echolucent carotid artery plaques into further risk strata. There was a negative correlation between GSM and FDG uptake in carotid artery plaques, and as seen in Figure 2, the main proportion of echorich plaques (high GSM) tended to show low FDG uptake, whereas echolucent plaques (low GSM) exhibited a wide range of FDG uptake values. The positive correlation found between CD68 expression and FDG uptake supports previous findings, and the evidence for the ability of FDG PET to depict inflammation in atherosclerosis is accumulating (12–14,16).

Ultrasound has largely replaced previous conventional contrast angiography and is a cost-effective way of screening patients. It supplies the reader with information about the degree of stenosis and plaque morphology, hence stability. However, several problems in assessing ultrasonographic plaque morphology have prevented this imaging method from reaching the level of clinical decision-making. Objectivity is hampered because the 2-dimensional nature of the ultrasound image leaves quantification of echolucent areas difficult, and areas are left unattended because of the shadowing from calcified portions of the plaques (4,5).

Computerized standardization of the ultrasound images has proven to overcome some of the subjectivity in morphology assessment, and the GSM analysis has proven to identify subgroups of patients with carotid plaques with a relative higher risk of cerebral events (8,17). Echolucency in plaques may reflect lipid deposits, hemorrhage, or necrotic debris (18–20). Although morphological traits of the vulnerable plaque can be identified, ultrasound does not reveal whether the plaque is stabilizing or actually metabolically active with inflammatory activity.

Our group (13) has previously shown that the PET-identifiable inflammation is also associated with molecular overexpression of enzymes known to have a role in the degrading processes of the plaque extracellular matrix. The combination of echolucency and high FDG uptake may thus identify the vulnerable plaque with high sensitivity. Considering the availability and the high costs of PET/CT as compared with ultrasound, it is likely that a clinical implementation of PET/CT for identification of high-risk patients could supplement rather than substitute ultrasound morphology investigations.

In our small population, only the PET scan demonstrated a significant difference between the symptomatic and the asymptomatic plaques, suggesting that PET is more sensitive than ultrasound in identifying vulnerable plaques. Results from the paired test in patients with bilateral plaques indicated that plaque FDG uptake was truly plaque dependent rather than patient dependent (greater FDG uptake on the symptomatic side). There was, however, a substantial overlap between the 2 groups, reflecting the limitation in using symptoms as a surrogate marker for inflammation. This limitation also was evident from the large spread in CD68 activity found within the symptomatic plaques alone. Studies that include gene expression analyses in plaques from asymptomatic patients are warranted in addition to larger studies investigating the consistency of our findings as well as the

expected high risk of ipsilateral stroke in patients with echolucent and high FDG uptake plaques.

Interobserver and intraobserver reproducibility of both PET and GSM have previously been investigated, and the numerical values for asymptomatic and symptomatic plaques we found were similar to previous reports (4,21). In our work, GSM values were generally low, probably reflecting the systemic nature of atherosclerotic activity in a population in which all patients had recent symptoms.

CONCLUSIONS

The use of FDG PET reveals inflammation in carotid artery plaques. Echolucent plaques exhibit a wide range of inflammatory activity, whereas echorich plaques demonstrate little inflammatory activity, and FDG PET may be useful for the stratification of echolucent plaques. Larger clinical trials will be needed to fully understand the benefit of additional PET/CT imaging in patients with carotid artery stenosis.

Reprint requests and correspondence: Dr. Martin Græbe, Department of Vascular Surgery, Rigshospitalet RK 3111, Blegdamsvej 9, DK-2100 Copenhagen, Denmark. *E-mail: martin.graebe@rh.regionh.dk.*

REFERENCES

1. Rothwell PM, Eliasziw M, Gutnikov SA, Warlow CP, Barnett HJ. Endarterectomy for symptomatic carotid stenosis in relation to clinical subgroups and timing of surgery. Lancet 2004;363:915–24.

2. Nicolaides AN, Kakkos SK, Griffin M, et al. Severity of asymptomatic carotid stenosis and risk of ipsilateral hemispheric ischaemic events: results from the ACSRS study. Eur J Vasc Endovasc Surg 2005;30:275–84.

3. Randomised trial of endarterectomy for recently symptomatic carotid stenosis: final results of the MRC European Carotid Surgery Trial (ECST). Lancet 1998;351:1379–87.

4. Sabetai MM, Tegos TJ, Nicolaides AN, Dhanjil S, Pare GJ, Stevens JM. Reproducibility of computer-quantified carotid plaque echogenicity: can we overcome the subjectivity? Stroke 2000;31:2189–96.

5. Fosse E, Johnsen SH, Stensland-Bugge E, et al. Repeated visual and computer-assisted carotid plaque characterization in a longitudinal population-based ultrasound study: the Tromso study. Ultrasound Med Biol 2006;32:3–11.

6. Mathiesen EB, Bonaa KH, Joakimsen O. Echolucent plaques are associated with high risk of ischemic cerebrovascular events in carotid stenosis: the tromsø study. Circulation 2001;103:2171–5.

7. Gronholdt ML, Nordestgaard BG, Bentzon J, et al. Macrophages are associated with lipid-rich carotid artery plaques, echolucency on B-mode imaging, and elevated plasma lipid levels. J Vasc Surg 2002;35:137–45.

8. Gronholdt ML, Nordestgaard BG, Schroeder TV, Vorstrup S, Sillesen H. Ultrasonic echolucent carotid plaques predict future strokes. Circulation 2001;104:68–73.

9. Basu S, Zhuang H, Torigian DA, Rosenbaum J, Chen W, Alavi A. Functional imaging of inflammatory diseases using nuclear medicine techniques. Semin Nucl Med 2009;39:124–45.

10. Warburton L, Gillard J. Functional imaging of carotid atheromatous plaques. J Neuroimaging 2006;16:293–301.

11. Vallabhajosula S, Fuster V. Atherosclerosis: imaging techniques and the evolving role of nuclear medicine. J Nucl Med 1997;38:1788–96.

12. Rudd JHF, Warburton EA, Fryer TD, et al. Imaging atherosclerotic plaque inflammation with [18F]-fluorodeoxyglucose positron emission tomography. Circulation 2002;105:2708–11.

13. Graebe M, Pedersen SF, Borgwardt L, Højgaard L, Sillesen H, Kjær A. Molecular pathology in vulnerable carotid plaques: correlation with [18]-fluorodeoxyglucose positron emission tomography (FDG PET). Eur J Vasc Endovasc Surg 2009;37:714–21.

14. Tawakol A, Migrino RQ, Bashian GG, et al. In vivo 18F-fluorodeoxyglucose positron emission tomography imaging provides a noninvasive measure of carotid plaque inflammation in patients. J Am Coll Cardiol 2006;48:1818–24.

15. Grant EG, Benson CB, Moneta GL, et al. Carotid artery stenosis: gray-scale and Doppler US diagnosis—Society of Radiologists in Ultrasound Consensus Conference. Radiology 2003;229:340–6.

16. Font MA, Fernandez A, Carvajal A, et al. Imaging of early inflammation in low-to-moderate carotid stenosis by 18-FDG-PET. Front Biosci 2009;14:3352–60.

17. Nicolaides AN, Kakkos SK, Griffin M, et al. Effect of image normalization on carotid plaque classification and the risk of ipsilateral hemispheric ischemic events: results from the asymptomatic carotid stenosis and risk of stroke study. Vascular 2005;13:211–21.

18. AbuRahma AF, Kyer 3rd PD, Robinson PA, Hannay RS. The correlation of ultrasonic carotid plaque morphology and carotid plaque hemorrhage: clinical implications. Surgery 1998;124:721–6; discussion 726–8.

19. Gronholdt ML, Wiebe BM, Laursen H, Nielsen TG, Schroeder TV, Sillesen H. Lipid-rich carotid artery plaques appear echolucent on ultrasound B-mode images and may be associated with intraplaque haemorrhage. Eur J Vasc Endovasc Surg 1997;14:439–45.

20. Carotid artery plaque composition—relationship to clinical presentation and ultrasound B-mode imaging. European Carotid Plaque Study Group. Eur J Vasc Endovasc Surg 1995;10:23–30.

21. Russell DA, Wijeyaratne SM, Gough MJ. Changes in carotid plaque echomorphology with time since a neurologic event. J Vasc Surg 2007;45:367–72.

Key Words: atherosclerosis ▪ FDG ▪ PET ▪ echolucent ▪ carotid plaque ▪ ultrasound.